

Analytical Methods

Accepted Manuscript



This is an *Accepted Manuscript*, which has been through the Royal Society of Chemistry peer review process and has been accepted for publication.

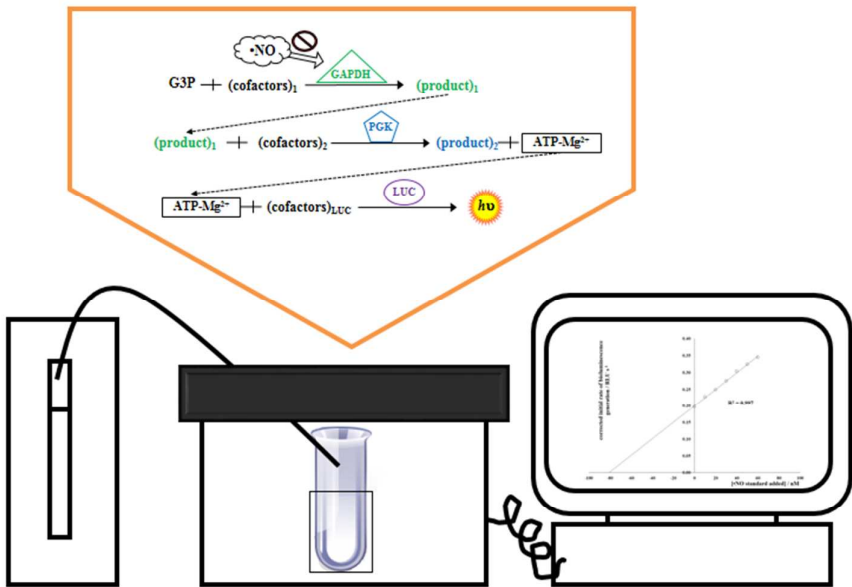
Accepted Manuscripts are published online shortly after acceptance, before technical editing, formatting and proof reading. Using this free service, authors can make their results available to the community, in citable form, before we publish the edited article. We will replace this *Accepted Manuscript* with the edited and formatted *Advance Article* as soon as it is available.

You can find more information about *Accepted Manuscripts* in the [Information for Authors](#).

Please note that technical editing may introduce minor changes to the text and/or graphics, which may alter content. The journal's standard [Terms & Conditions](#) and the [Ethical guidelines](#) still apply. In no event shall the Royal Society of Chemistry be held responsible for any errors or omissions in this *Accepted Manuscript* or any consequences arising from the use of any information it contains.

Table of contents entry

A fast, simple, sensitive and robust enzymatic method with bioluminescent detection for nitric oxide is presented



Nitric oxide quantitative assay by a glyceraldehyde 3-phosphate dehydrogenase/phosphoglycerate kinase/firefly luciferase optimized coupled bioluminescent assay

Simone M. Marques and Joaquim C.G. Esteves da Silva*

A novel optimized coupled bioluminescent assay for nitrogen monoxide free radical (nitric oxide, •NO), an important environmental and physiological molecule, is presented. The method is based on the reaction catalyzed by glyceraldehyde 3-phosphate dehydrogenase (GAPDH), whose product is used as a substrate for phosphoglycerate kinase (PGK), generating adenosine 5'-triphosphate (ATP), which is an essential cofactor for the firefly luciferase bioluminescent reaction. Inhibition of GAPDH by •NO hampers the coupled reactions, leading to a depletion of ATP and hence a decrease in the bioluminescent signal. Using diethylamine NONOate (DEA-NONOate) as the •NO donor, the assay was optimized through statistical experimental design methodology, namely Plackett-Burman (screening) and Box Behnken (optimization) designs. The optimized method requires 5 µL of sample *per* tube in a final reaction volume of 100 µL. It is linear in the range from 10 to 100 nM of •NO, with limits of detection and quantitation of 4 and 15 nM, respectively. Limitations in its application to biological samples, together with approaches to solve them, are discussed using human whole saliva and microalgae culture medium as examples.

Chemistry Research Center of the University of Porto (CIQ-UP), Department of Chemistry and Biochemistry, Faculty of Sciences, University of Porto, Campo Alegre St., w/n, Building FC2, 4169-007 Porto, Portugal. E-mail: jcsilva@fc.up.pt; Fax: +351 220 402 659; Tel: +351 220 402 569

Introduction

Nitrogen monoxide, commonly known as nitric oxide ($\bullet\text{NO}$), is a small gaseous and free radical molecule containing one unpaired electron with an enormous importance in the environmental, biological and pathological contexts.¹⁻⁴ It is mainly recognized as an atmospheric pollutant, along with its derivative nitrogen dioxide (NO_2), and as an intra- and extracellular signaling molecule with relevant roles in inflammatory, carcinogenic, cardiovascular, immune response, neurodegenerative and neurotransmission, and pain generation processes.¹⁻⁴

Methods for $\bullet\text{NO}$ detection and quantitation may be direct or indirect. In indirect methods, the $\bullet\text{NO}$ amount is estimated through its derivatives, nitrite (NO_2^-), nitrate (NO_3^-), or NO_2 . Assuming that all the $\bullet\text{NO}$ in a sample tends to be converted into the more stable products nitrate and nitrite, a widespread indirect method is the Griess test for nitrite.⁵ Nitrate may also be quantified by its previous conversion to nitrite, for example by using nitrate reductase. Although simple to perform, this methodology may not reflect the endogenous $\bullet\text{NO}$ content, which originates from nitric oxide synthase reactions with the amino acid L-arginine,² because other sources may affect the results, for example dietary intake.⁶ Other popular methods are based on fluorescence,⁷ ultraviolet-visible (UV-vis) spectrophotometry,⁸ electrochemical sensors,⁹⁻¹¹ chemiluminescence with ozone,^{12,13} spin trapping coupled to electron paramagnetic resonance (EPR) spectroscopy^{14,15} and membrane inlet mass spectrometry (MS).¹⁶ Recent approaches for $\bullet\text{NO}$ quantitation include the use of nanomaterials to create novel electrochemical sensors,¹⁷⁻²¹ the synthesis of novel fluorescent probes,^{22,23} the bioimaging of $\bullet\text{NO}$ in living cells and small animals^{23,24} and coupled enzymatic assays.²⁵ Those methods are in general highly sensitive, with limits of detection (LOD) varying from the nanomolar range, 0.31¹⁷ up to 95 nM,²¹ to the low micromolar range, 0.1²⁰ up to 3 μM .⁷ However, some problems are worthy to note. EPR and MS equipment are not portable, involve high costs of acquisition

and maintenance, and may require specialized personnel to operate. The dyes used in fluorescent and UV-vis methods may participate in side reactions, either reducing their free amount to react with $\bullet\text{NO}$ or leading to other fluorescent or coloured products which interfere with the assay.^{26,27} The use of nanomaterials is very promising, but some concerns regarding their toxicity are still under discussion.^{28,29} Lastly, most of the proposed new methods were not tested in real samples, nor they were subjected to optimization. In this paper, an optimized coupled bioluminescent assay for $\bullet\text{NO}$ will be presented.

Coupled enzymatic assays refer to analytical methods in which several enzymatic reactions, one of which using the desired analyte, occur sequentially to generate a measurable signal.³⁰ A first reaction generates one product that will be used in a second coupled reaction as a substrate. The second reaction will generate another product that may be used as substrate in a third coupled reaction and so on, until a final product that is measured. When the measured product are photons, the assay is termed coupled bioluminescent assay.³⁰ Coupled enzymatic assays are useful when the enzymatic reaction consuming or producing the desired analyte does not lead to an easily measurable product. Furthermore, they may lead to signal amplification. On the other hand, if one of the enzymes is inactivated, or the concentration of one of the reagents is too low, the coupling is hampered, which requires the careful evaluation of each enzyme and reagent prior to the assay.

In the present method, the first reaction of the coupling is catalyzed by glyceraldehyde 3-phosphate dehydrogenase (GAPDH), producing 1,3-bisphosphoglycerate (1,3-BPG) in the presence of its substrate, glyceraldehyde 3-phosphate (G3P), and the cofactors β -nicotinamide adenine dinucleotide (NAD^+) and phosphate ions (Pi) (Scheme 1). The product, 1,3-BPG, is used as a substrate for phosphoglycerate kinase (PGK), producing 3-phosphoglycerate (3-PG). In the course of this reaction its cofactor, adenosine 5'-diphosphate (ADP), is phosphorylated into adenosine 5'-triphosphate (ATP), which is an essential cofactor for the bioluminescent

reaction catalyzed by firefly luciferase (LUC). In the presence of ATP, molecular oxygen (O₂) and its natural substrate, firefly D-luciferin (D-LH₂), LUC generates adenosine 5'-monophosphate (AMP), inorganic pyrophosphate (PPi), carbon dioxide (CO₂), oxyluciferin and photons of visible light which are recorded in a luminometer. •NO is known to inhibit GAPDH, presumably by acting on a thiol group from an enzyme's active site cysteine, albeit this is still under discussion.³¹⁻³⁶ By inhibiting GAPDH, the production of ATP is impaired, decreasing the light output.

(Z)-1-[N,N-diethylamino]diazen-1-ium-1,2-diolate (diethylamine NONOate, DEA-NONOate) was used as a •NO donor. NONOates are prepared in alkaline solutions and, by lowering the pH, under defined temperature and concentration conditions, they dissociate to the free amino and •NO according to a defined stoichiometry. These features make them a versatile and convenient choice for an ever greater number of studies.^{37,38}

Experimental

Note. All experiments were performed at room temperature (approximately 20 °C). Concentration values are final.

Reagents and solutions

The enzymes (Table 1) and the reagents 4-(2-hydroxyethyl)piperazine-1-ethanesulfonic acid (HEPES, product code H3375), G3P (DL-glyceraldehyde 3-phosphate solution, product code G5251), NAD⁺ (sodium salt, from *Saccharomyces cerevisiae*, product code N0632), DEA-NONOate (sodium salt hydrate crystalline, product code D184), ADP (potassium salt, from a bacterial source, desiccate, product code A5285), ATP (disodium salt hydrate, from a bacterial

source, product code A2383), D-LH₂ (synthetic free acid, product code L9504), glycine (ACS reagent, $\geq 98.5\%$, product code 410225) and magnesium chloride (MgCl₂, hexahydrate, product code 63064) were purchased from Sigma-Aldrich® (Steinheim, Germany). Sodium sulfate (Na₂SO₄) was obtained from Pronalab (Lisbon, Portugal). Sodium hydroxide (NaOH) was purchased from Moura Drugstore (Porto, Portugal). Sodium dihydrogen phosphate monohydrate (NaH₂PO₄·H₂O, *pro analysi*) was obtained from Merck (Darmstadt, Germany). Nitrogen (Alphagaz™ Smartop N₂) was obtained from Air Liquide Portugal (Algés, Portugal).

All reagents were used without further purification. Stock solutions of the enzymes were prepared by dissolving the whole content of the flasks in HEPES buffer 0.5 M, pH 7.5, with the exception of PGK, which was purchased as an ammonium sulfate suspension.

HEPES was prepared by dissolving the corresponding mass in deionized water, and the pH was adjusted to 7.5 using a NaOH 10 M solution. Phosphate buffer 150 mM, pH 6.9 was prepared by dissolving the corresponding mass of NaH₂PO₄·H₂O in deionized water and adjusting the pH to 6.9 using a NaOH 10 M solution. G3P was purchased as an aqueous solution. Stock solutions of NAD⁺, ADP, ATP, MgCl₂ and glycine were prepared in deionized water without pH adjustment. D-LH₂ stock solutions were prepared in deionized water with intense stirring for about 1 hour, protected from the air and from the light. Concentration was confirmed by UV-vis spectrophotometry using an Unicam Helios γ spectrophotometer (Cambridge, U.K.) and considering a molar extinction coefficient of 18,200 L mol⁻¹ cm⁻¹ at the maximum wavelength (λ_{max}) of 327 nm.³⁹ For the preparation of Na₂SO₄ stock solutions, the salt was previously heated in an oven at 100 °C for 12 hours, then transferred to a desiccator filled with cobalt (II) chloride until it cooled to room temperature and the corresponding mass was weighted and dissolved in deionized water. DEA-NONOate solutions were freshly prepared by dissolving the corresponding mass in a NaOH 10 mM solution previously bubbled with a nitrogen stream in capped polypropylene tubes. Concentration was confirmed by UV-

vis spectrophotometry using the molar extinction coefficient of 6,500 L mol⁻¹ cm⁻¹ at λ_{max} 250 nm, according to the manufacturer's information. Prior to the assays, solutions were diluted 1:20 in phosphate buffer 50 mM, pH 6.9 (Pi) for 20 minutes at room temperature, protected from air, to allow the release of •NO. Concentrations after release were calculated by considering a ratio of 1.5 moles of •NO *per* parent compound, according to the manufacturer's information

To ensure that the same conditions were achieved throughout the work, and also to avoid multiple freezing-thawing cycles, stock solutions were prepared in large volumes, aliquoted in small volumes and stored at -20 °C with the exception of PGK, which was stored at 2 °C.

Experimental designs

Experimental designs were created using The Unscrambler® version 9.2 from CAMO (Oslo, Norway). Screening designs were created using Plackett-Burman designs with eleven continuous variables at two levels and one nondesign (response) variable, which was set as •NO 5 nM [electronic supplementary information (ESI), 'Experimental' and Table S1]. For the experimental procedure, it was chosen one replication *per* experiment and three centre (control) experiments, with a total of twelve testing experiments plus the three control experiments. Optimization designs were created using Box Behnken designs with five continuous variables at two levels and one nondesign variable, which was set as •NO 5 nM (ESI, 'Experimental' and Table S1). For the experimental procedure, it was chosen one replication *per* experiment and five centre experiments, with a total of forty testing experiments plus the five control experiments.

Coupled bioluminescent assays

Optimized protocol. Coupled bioluminescent assays were performed using a homemade luminometer with a Hamamatsu HCL35 photomultiplier tube (Middlesex, N.J., U.S.A) inside a light-tight dark chamber coupled to a Crison MicroBU 2030 automatic microburette (Barcelona, Spain) equipped with a 2.5-mL Hamilton GASTIGHT® 1002 glass syringe (Bonaduz, Switzerland).

The stock solutions of reagents were diluted in deionized water, DEA-NONOate standard solutions were diluted in NaOH 10 mM, and the enzymes were diluted in HEPES buffer 0.5 M, pH 7.5, and kept on ice until use.

Reaction mixtures with the composition and volumes indicate in Scheme 2 were prepared in capped polypropylene tubes. Five microliters of DEA-NONOate standard solutions was transferred to transparent test tubes, the reaction mixture was added and the tubes were introduced into the dark chamber, one at a time. The baseline register by the equipment was turned on, at an integration interval of 1 second. After 30 seconds, 30 μL of PGK 0.011 $\mu\text{g mL}^{-1}$ was injected from the automatic burette. The light output was recorded for 3 minutes after injection. A schematic representation of these steps is presented in Scheme 2.

Method figures of merit. Preliminary calibration curves were made according to the procedure described in subsection ‘Optimized protocol’ using DEA-NONOate standards corresponding to $\bullet\text{NO}$ concentrations from 0 to 1,000 μM (ten experimental points for each curve, each point measured in triplicate). To evaluate precisely the linear range of the method, calibration curves were made using DEA-NONOate standards corresponding to $\bullet\text{NO}$ concentrations from 0 to 100 nM (eleven experimental points for each curve, each point measured in triplicate). For the estimation of the method’s repeatability, assays were made with DEA-NONOate standards corresponding to $\bullet\text{NO}$ concentrations of 10, 50 and 100 nM (each concentration measured in quintuplicate in each assay).

Samples' assays.

Sample handling and maintenance. Resting whole saliva was freshly collected using a swab at least 90 minutes after a morning meal and stored in capped polypropylene tubes. A laboratorial culture of *Chlorella vulgaris* was inoculated in a 250-mL glass Erlenmeyer previously boiled in deionized water with Z8 medium, constant aeration and a 16h light / 8h dark photoperiod. Freshly prepared culture medium was added to the Erlenmeyer once a week to replace evaporated medium. Aliquots were taken when the microalgae reached the exponential grown phase.

•NO quantitation. Assays were performed using the conditions described in subsection 'Optimized protocol'. Using the method of standard additions, 5.00 µL aliquots of sample were added to 5.00 µL of DEA-NONOate standards corresponding to •NO concentrations from 0 to 60 nM (seven experimental points for each curve, each point measured in triplicate). The volume of PGK was reduced to 25 µL. A blank, in which the sample plus DEA-NONOate standard was replaced with deionized water, was measured in triplicate.

Statistical analysis.

Experimental designs. Data obtained from the experimental designs was analyzed using The Unscrambler® software. For the Plackett-Burman screening design, an analysis of effect was performed. Results were expressed as effects overview, using the significance testing method Center. For the Box Behnken optimization design, a response surface analysis, which includes a two-way analysis of variance (ANOVA) table, residuals calculation and response surface, was applied. From the ANOVA table, the analyzed parameters were the summary (evaluation of the global model), the variable (evaluation of the significance of each of the variables tested), the model check (evaluation of the global quadratic model) and the lack of fit (degree of misfitting of the experimental data to the model). All those parameters were

evaluated through their F -ratios and the corresponding p -values. Regarding the variables, the b -coefficients and their corresponding standard errors were also taken into account. A p -value <0.05 was considered as statistically significant.

Coupled bioluminescent assays.

Note. Data treatment and calculations were performed with a Microsoft® Excel® spreadsheet.

General calculations. Quantitation of $\bullet\text{NO}$ is achieved through calibration curves, set up by the method of least squares, by plotting the initial rate of bioluminescence generation as a function of the concentration of $\bullet\text{NO}$ standard solutions. The initial rate of bioluminescence generation was obtained by plotting the recorded bioluminescence, after the subtraction of the baseline, as a function of time (in seconds), and calculating the slope of the linear portion of the plot, which corresponds to the first 60 seconds of reaction (Fig. 1A). Baseline was defined as the average recorded bioluminescence prior to the injection of PGK, which corresponds to the first 30 seconds of record. Each experimental point in the calibration curves is presented as mean \pm standard deviation (SD) ($n = 3$) (fig. 2). In Fig. 1B, differences among the values were evaluated by one-way ANOVA followed by the Dunnett's multiple-comparison test.

Method figures of merit. The method figures of merit linear range, LOD and limit of quantitation (LOQ) were obtained through calibration curves settled by the method of least squares (Fig. 2). LOD and LOQ were calculated using the following criteria: $\text{LOD} = (a + 3S_{y/x})$ and $\text{LOQ} = (a + 10S_{y/x})$, in which a is the intercept of the calibration curves and $S_{y/x}$ is the random error in the y -direction.⁴⁰ Precision was expressed as relative standard deviation (RSD) calculated with the expression $(\text{SD} / \text{mean}) \times 100$ ($n = 3$), of two independent assays.

$\bullet\text{NO}$ quantitation. The $\bullet\text{NO}$ content in samples was assayed by the method of standard additions. Curves were set up by calculating and plotting the corrected initial rate of

bioluminescence generation using the expression {corrected initial rate of bioluminescence generation = [average signal of blank (in triplicate) – average signal of sample plus DEA-NONOate standard (in triplicate)]/average signal of blank}, wherein the blank was prepared without DEA-NONOate addition and without sample (Fig. 3). The concentration of •NO was given as the ratio between the intercept and the slope of the regression line in Fig. 3, and expressed as •NO concentration ± 95% confidence limits (95% CL) of the concentration ($n = 3$), for two independent assays.

Results and discussion

Preliminary assays

The proposed method is based on the coupling of three enzymatic reactions, with the detection based on the linear decrease of bioluminescent signal due to a reduction in ATP generation. Before proceeding to its optimization and characterization, preliminary assays were made.

The activity of both of the enzymes GAPDH and PGK, as well as the release of •NO from DEA-NONOate, were evaluated through UV-vis spectrophotometry. The GAPDH catalyzed reaction produces NADH + H⁺ (Scheme 1), which presents an absorption band at λ_{max} 340 nm. The continuous production of NADH + H⁺ leads to an increase in absorbance monitored at this wavelength. In the absence of GAPDH and the presence of PGK (blank GAPDH), the absorbance is constant and the values are reduced to a minimum, indicating no production of NADH + H⁺ (ESI, ‘Experimental’ and Fig. S1). In the presence of GAPDH and the absence of PGK (blank PGK), the absorbance is still constant, but with values about ten times higher. This may indicate that some NADH + H⁺ was produced by GAPDH, but because PGK was not available to further drive the reaction, the concentration remained constant. Only with both GAPDH and PGK in the reaction mixture (test) an increase in absorbance over time

was observed, indicating continuous production of $\text{NADH} + \text{H}^+$. It was then confirmed the integrity and correct coupling of the enzymes.

Intact DEA-NONOate has an absorption band at λ_{max} 250 nm. When the molecule dissociates to the free amine and $\bullet\text{NO}$, the absorbance registered at this wavelength decreases over time. In ESI, 'Experimental' and Fig. S2, a representative DEA-NONOate decomposition spectrum of a solution corresponding to 10 μM of $\bullet\text{NO}$ diluted 1:20 in Pi is shown. The compound is completely dissociated within 15 minutes, as the absorbance reaches zero, indicating that the DEA-NONOate solution is in good experimental conditions.

It is mandatory to avoid exogenous ATP, because it will interfere with the assay. Furthermore, because the method involves decrease in light detection, it is important to verify that this is not due to an inhibitory effect of some of the reagents or enzymes on LUC. With this aim, two bioluminescent assays were devised. One of the assays aimed to verify any interference of the emitted light in the presence of reagents or enzymes compared to a control without them. The other was done without exogenously added ATP, so that any produced light would be due to ATP contamination within reagents or enzymes. Results showed no contamination of ATP in reagents and enzymes (ESI, 'Experimental' and Table S2). The maximum value registered was from ADP but, even so, it was only 0.71% of the control. Regarding the influence on LUC activity, it was detected a slightly inhibition of light production from Pi (90% of the light emitted by the control) and DEA-NONOate (93% of the light emitted by the control) (ESI, 'Experimental' and Fig. S3). Because pure NaOH was not interfering (ESI, Fig. S3), the effect was due to DEA-NONOate itself or some $\bullet\text{NO}$ released upon contact to LUC, since the enzyme is at a lower pH value (7.5) compared to the DEA-NONOate solution (about 12). It was reported that $\bullet\text{NO}$ could inhibit the transcription of the *luc* gene,⁴¹ but no reports of its action on the mature enzyme is available, to the best of our knowledge. Furthermore, it was demonstrated that $\bullet\text{NO}$ activates the flashing of fireflies *in vivo*, but only

through the inhibition of O₂ usage by mitochondria in photocytes, and not due to a direct action upon the enzyme.⁴²⁻⁴⁶ The inhibition of Pi was not expected, since this buffer is used in bioluminescent assays with LUC.⁴⁷ The effect may be due to the Pi-induced precipitation of Mg²⁺ cations.⁴⁸ Pi has three functions in this assay, as a source of phosphate ions for the coupled reactions, as a preferential buffer for GAPDH and as a medium for DEA-NONOate dissociation. Its substitution for another buffer with all these features was not possible. The last preliminary assay was to evaluate, by luminometry, the enzymatic reactions coupling and the effect of •NO on GAPDH (Fig. 1). Light is produced in the presence of the complete reaction mixture and absence of both •NO and ATP (Fig. 1A). By eliminating GAPDH, no light is produced, confirming that ATP is produced *via* the coupled reactions. Addition of •NO significantly reduced ($p < 0.05$) the light output. At 1 nM •NO, light is reduced to about 93% of that of the control, and the percentage is reduced to only 25% when •NO concentration is raised to 1 μM (Fig. 1B). However, when raising again the •NO concentration to 1 mM, the percentage remains at 25% of the control, probably due to enzyme saturation at the tested concentrations of reagents and enzymes (Fig. 1B). Thus, the possible working range for •NO quantitation, using the method's chosen conditions, lies between the nanomolar up to the low micromolar range.

Experimental designs

The method was optimized using an experimental design methodology. The overall optimization process included two steps, a screening, to identify which factors have statistically the most influence on the method's response, and the subsequent determination of the levels at which these factors must be kept to optimize the method's response. Taking into account the various reagents and steps in the method, eleven factors were initially selected for screening and a Plackett-Burman design was selected (ESI, 'Experimental' and Table S1). The choice for

D-LH₂ and LUC concentration values was based on solubility constraints of D-LH₂ and the costs of the enzyme, respectively. The concentrations of the remaining reagents and enzymes were based on the 'Enzymatic Assay of 3-Phosphoglycerate Phosphokinase (EC 2.7.2.3) from Baker's Yeast' protocol by the manufacturer.

On the basis of the preliminary results, the percentage of Pi was reduced from 45% of Pi (v/v) to 25% (ESI, 'Experimental'). Likewise, when testing the effect of DEA-NONOate on LUC activity, a relatively large volume of this solution was tested, 20 μ L in a 100- μ L final reaction volume, or a 1:5 dilution factor (ESI, 'Experimental'). However, the \bullet NO releasing conditions in the experimental design assay require a higher dilution factor: DEA-NONOate is diluted 1:20 in Pi, then 5 μ L of this solution is assayed in a final reaction volume of 100 μ L. These conditions are expected to reduce the interfering effect on LUC. Because PGK was injected using an automatic burette, it was not possible to largely reduce its volume, so that the volume of PGK was altered from 50 μ L in the preliminary assay to 30 μ L (ESI, 'Experimental'). Furthermore, the time of reaction was reduced from 10 minutes in the preliminary assay to 3 minutes and 30 seconds in the experimental design assay, because it was verified that a direct proportion of light production over time only occurs in the first minutes of reaction. Results showed that, in the presence of 5 nM of \bullet NO and using the testing method Center, the concentrations of Pi (--), G3P (-), ADP (++), MgCl₂ (+), and the pre-incubation time (-) were likely the most significant factors (Table 2). The factors with minus signal exerted a negative influence, that is, the higher their value, the lower was the response, whereas the plus signal indicated that the higher their value, the higher was the response. The number of minus or plus signals indicates the extension of their effects. Overall, the factors that could boost light generation (ADP and MgCl₂) revealed a positive effect, whereas those which could impair ATP generation (preincubation time) had a negative one. Once again, the negative influence of Pi

over the method's response was verified, together with a negative effect from G3P, which does not have a clear pattern in either enhancing or reducing the ATP generation.

With this information, a Box Behnken optimization design was built to uncover the best Pi, G3P, ADP and MgCl₂ concentrations, together with the best preincubation time, and to discover if their interactions are also important for the method's response. The remaining factors were kept at their intermediary concentration. From the ANOVA table (Table 3), it was verified that only the ADP concentration ([ADP], C), the preincubation time (E) and the quadratic factor preincubation time x preincubation time (EE) are important factors, showing significant *F*-ratios ($p < 0.05$). According to its *F*-ratio, the model obtained from the experimental measurements is significant ($p < 0.05$). Furthermore, the lack of fit of the model is not significant ($p > 0.05$), which confirms the validity of the optimization design model. The response surface curve (ESI, 'Experimental' and Fig. S4) shows that the concentration of ADP should be kept at the highest value tested (0.36 mM) to obtain the maximum signal (bioluminescence emission), whereas the preincubation time should be kept to a minimum. Taking these into consideration, the concentrations were kept to the central values tested in the screening design with the exceptions of ADP, whose concentration was raised to 0.3 mM, and Pi which, although not considered a significant factor according to the ANOVA results, the concentration was lowered to 30 mM to avoid any inhibitory effect. To the sake of simplicity, preincubation was excluded from the optimized protocol.

Optimized coupled bioluminescent assays

Using the optimized conditions, the coupled bioluminescent assay was characterized in terms of linear range, LOD and LOQ and repeatability at low, medium and high concentrations of •NO.

The preliminary assay (Fig. 1) indicated that the method is responsive in the nano- to low micromolar range, yet the precise interval was not known. To account for it, exploratory calibration curves in a relatively enlarged interval (0 to 1,000 μM of $\bullet\text{NO}$) were performed (Fig. 2). It was verified that a linear trend occurs between 0 to 100 nM (Fig. 2, inset). Novel curves were set up in this interval, to which LOD and LOQ were calculated as 4 and 15 nM of $\bullet\text{NO}$, respectively. The repeatability of the method was estimated from the relative standard deviation, and showed values of 3.84% at 20 nM, 5.70% at 50 nM and 4.28% at 100 nM of $\bullet\text{NO}$ (ESI, 'Experimental' and Fig. S5).

These results demonstrate the method's applicability to estimate the $\bullet\text{NO}$ releasing potential of $\bullet\text{NO}$ donors such as DEA-NONOate in aqueous solutions. However, to enhance its scope, and hence be attractive to a larger number of analysts, a method should also be suitable to complex samples, such as cellular suspensions. Before testing such samples, a survey of potential drawbacks was made.

Besides $\bullet\text{NO}$, GAPDH can be inhibited by thiol oxidizing agents, namely hydrogen peroxide.⁴⁹ Little interference is expected from aqueous samples, but biological samples can interfere. ATP is ubiquitous in biological samples, and it is a major interfering in this bioluminescent method. Furthermore, with the exceptions of LUC and D-LH₂, the reagents and enzymes in this method are also abundant in cells. Centrifugation may be used to separate cells, which contain the bulk of biological compounds, from supernatant. The remaining ATP may be removed through enzymatic reactions that consume or degrade ATP. An example of such reaction is catalyzed by ATP sulfurylase in the presence of sulfate ions (SO_4^{2-}), giving adenosine 5'-phosphosulfate (APS) and PPi (eqn (1)).⁵⁰



By its turns, PPi must also be removed, not only to favor the consumption of ATP but also because PPi interferes with the bioluminescent reaction.⁵¹ This can be achieved by adding inorganic pyrophosphatase (PPase) to the medium (eqn (2)).⁵⁰



It must be taken into account, however, that extensive manipulation and harsh laboratorial procedures may be stressful to cells, leading to the release of intracellular ATP to the medium, as well as altering the production of •NO, either below or above normal values. Another approach consists of using the method of standard additions.⁴⁰ This is a type of data analysis in which several standards of rigorously known concentration of the analyte are added to all but one aliquots of samples. The signal is measured for all samples and a calibration curve is obtained. The original concentration of the analyte is obtained by reading the absolute value of the *x*-intercept for the zero signal. The method has some disadvantages, namely it is more time-consuming because every sample has to have its own curve, it demands larger quantities of samples and most of the time it is not possible to separate samples from the standards after the procedure. Nevertheless, it is the method of choice for biological samples where matrix effects often occur.

As a proof-of-principle, human whole saliva and microalgae culture medium were assayed using this new optimized method. These samples were chosen as examples of a clinical application, in the case of saliva, and as an important technological and biological product, the microalgae. The content of ATP in these samples was estimated as 916 nM for saliva and 864 nM for microalgae culture medium (ESI, ‘Experimental’ and Fig. S6). After the reaction with ATP sulfurylase and PPase (ESI, ‘Experimental’), the ATP content dropped to 19 nM in saliva

and 7 nM in microalgae culture medium (ESI, 'Experimental'). Samples were then assayed using the method of standard additions. The results obtained using this methodology indicate a linear relationship between the concentration of added •NO standards and the bioluminescent light emission (Fig. 3, example for microalgae culture medium). Furthermore, no interference in LUC activity was observed (ESI, 'Experimental'). The •NO content was estimated to be 60.79 ± 7.13 nM for saliva and 80.75 ± 7.39 nM in microalgae culture medium.

It is evident that these and other drawbacks must be solved before the quantitative application of this methodology to complex samples. Nonetheless, these preliminary results also indicate that this goal can be accomplished with a careful planning. When this stage is reached, a comparison study between this method and others described in the literature will be paramount.

Conclusions

This paper presented the establishment of an optimized coupled bioluminescent assay for •NO quantitation. The novelty of this assay is not only the use of coupled enzymatic reactions with detection by luminometry, but also its optimization based on an experimental design methodology. This optimized method is sensitive, safe, simple to perform and economic despite the use of several reagents and enzymes because of their reduced volumes. All reagents and enzymes are commercially available, do not need further purification prior to use and their solutions are stable for several months when stored at -20 °C. Although we used a single-tube luminometer, the method is applicable to multiplate assay. Besides its application to aqueous NONOates solution studies, an exploratory application in biological samples was presented and its drawbacks were discussed.

Acknowledgements

Simone M. Marques wants to thank a Ph.D. scholarship (reference SFRH/BD/65109/2009), co-funded by the European Social Fund (*Fundo Social Europeu, FSE*), through *Programa Operacional Potencial Humano-Quadro de Referência Estratégico Nacional (POPH-QREN)*, and by national funds from the Ministry of Education and Science through the Portuguese *Fundação para a Ciência e a Tecnologia, I.P. (FCT, I.P.)*.

References

- 1 A. Butler and R. Nicholson, *Life, Death and Nitric Oxide*, The Royal Society of Chemistry, Padstow, 2003.
- 2 D.S. Brecht, *Free Radic. Res.*, 1999, **31**, 577-596.
- 3 L. Lamattina, C. García-Mata, M. Graziano and G. Pagnussat, *Annu. Rev. Plant Biol.*, 2003, **54**, 109-136.
- 4 D.D. Thomas, L.A. Ridnour, J.S. Isenberg, W. Flores-Santana, C.H. Switzer, S. Donzelli, P. Hussain, C. Vecoli, N. Paolocci, S. Ambs, C.A. Colton, C.C. Harris, D.D. Roberts and D.A. Wink, *Free Radic. Biol. Med.*, 2008, **45**, 18-31.
- 5 D.J.D. Nicholas and A. Nason, *Methods Enzymol.*, 1957, **3**, 981-984.
- 6 M. Gilchrist, P.G. Winyard and N. Benjamin, *Nitric Oxide-Biol. Chem.*, 2010, **22**, 104-109.
- 7 E.F.C. Simões, J.M.M. Leitão and J.C.G. Esteves da Silva, *J. Fluoresc.*, 2013, **23**, 681-688.

- 1
2
3 8 L.A. Ridnour, J.E. Sim, M.A. Hayward, D.A. Wink, S.M. Martin, G.R. Buettner and
4 D.R. Spitz, *Anal. Biochem.*, 2000, **281**, 223-229.
5
6
7
8 9 S. Borgmann, *Anal. Bioanal. Chem.*, 2009, **394**, 95-105.
9
10 10 R. Trouillon, *Biol. Chem.*, 2012, **394**, 17-33.
11
12 11 F. Bedioui and S. Griveau, *Electroanalysis*, 2013, **25**, 587-600.
13
14 12 A. Fontijn, A.J. Sabadell and R.J. Ronco, *Anal. Chem.*, 1970, **42**, 575-579.
15
16 13 J.N. Bates, *Neuroprotocols*, 1992, **1**, 141-149.
17
18 14 K. Tsuchiya, M. Takasugi, K. Minakuchi and K. Fukuzawa, *Free Radic. Biol. Med.*,
19 1996, **21**, 733-737.
20
21
22
23 15 E. van Faassen and A. Vanin, *Nitric Oxide-Biol. Chem.*, 2006, **15**, 233-240.
24
25 16 D.N. Silverman and C. Tu, *Methods. Mol. Biol.*, 2011, **704**, 105-114.
26
27 17 P. Kannan and S.A. John, *Electrochim. Acta*, 2010, **55**, 3497-3503.
28
29 18 T. Madasamy, M. Pandiaraj, M. Balamurugan, S. Karnewar, A.R. Benjamin, K. A.
30 Venkatesh, K. Vairamani, S. Kotamraju and C. Karunakaran, *Talanta*, 2012, **100**, 168-
31 174.
32
33 19 C.M. Yap, G.Q. Xu and S.G. Ang, *Anal. Chem.*, 2013, **85**, 107-113.
34
35 20 X. Zan, Z. Fang, J. Wu, F. Xiao, F. Huo and H. Duan, *Biosens. Bioelectron.*, 2013, **49**
36 71-78.
37
38 21 Wang, P. Hu, X. Deng, F. Wang and Z. Chen, *Biosens. Bioelectron.*, 2013, **50**, 57-61.
39
40 22 N. Kumar, V. Bhalla and M. Kumar, *Coord. Chem. Rev.*, 2013, **257**, 2335-2347.
41
42 23 J.-B. Chen, H.-X. Zhang, X.-F. Guo, H. Wang and H.-S. Zhang, *Anal. Bioanal. Chem.*
43 DOI 10.1007/s00216-013-7177-6.
44
45 24 H. Hong, J. Sun and W. Cai, *Free Radic. Biol. Med.*, 2009, **47**, 684-698.
46
47 25 Y.Y. Woldman, J. Sun, J.L. Zweier and V.V. Khramtsov, *Free Radic. Biol. Med.*, 2009,
48 **47**, 1339-1345.
49
50
51
52
53
54
55
56
57
58
59
60

- 1
2
3 26 X. Zhang, W.-S. Kim, N. Hatcher, K. Potgieter, L.L. Moroz, R. Gillette and J.V.
4
5 Sweedler, *J. Biol. Chem.*, 2002, **277**, 48472-48478.
6
7
8 27 K. Uhlenhut and P. Högger, *Free Radic. Biol. Med.*, 2012, **52**, 2266-2275.
9
10 28 S. Sharifi, S. Behzadi, S. Laurent, M.L. Forrest, P. Stroeve and M. Mahmoudi, *Chem.*
11
12 *Soc. Rev.*, 2012, **41**, 2323-2343.
13
14 29 B. Pelaz, G. Charron, C. Pfeiffer, Y. Zhao, J.M. de la Fuente, X.-J. Liang, W.J. Parak
15
16 and P. del Pino, *Small*, 2013, **9**, 1573-1584.
17
18 30 M.J. Corey, *Coupled Bioluminescent Assays – Methods, Evaluations, and Applications*,
19
20 John Wiley and Sons, Hoboken, N.J., 2009.
21
22 31 S. Dimmeler, F. Lottspeich and B. Brüne, *J. Biol. Chem.*, 1992, **267**, 16771-16774.
23
24 32 S. Dimmeler and B. Brüne, *FEBS Lett.*, 1993, **315**, 21-24.
25
26 33 S. Mohr, J.S. Stamler and B. Brüne, *FEBS Lett.*, 1994, **348**, 223-227.
27
28 34 M. Itoga, M. Tsuchiya, H. Ishino and M. Shimoyama, *J. Biochem.*, 1997, **121**, 1041-
29
30 1046.
31
32 35 S. Mohr, H. Hallak, A. de Boitte, E.G. Lapetina and B. Brüne, *J. Biol. Chem.*, 1999,
33
34 **274**, 9427-9430.
35
36 36 K.A. Broniowska and N. Hogg, *Am. J. Physiol.-Heart Circul. Physiol.*, 2010, **299**,
37
38 H1212-H1219.
39
40 37 L.K. Keefer, R.W. Nims, K.M. Davies and D.A. Wink, *Methods Enzymol.*, 1996, **268**,
41
42 281-293.
43
44 38 Q. Li and J.R. Lancaster Jr., *Nitric Oxide-Biol. Chem.*, 2009, **21**, 69-75.
45
46 39 L.J. Bowie, *Methods Enzymol.*, 1978, **57**, 15-28.
47
48 40 J.N. Miller and J.C. Miller, *Statistics and Chemometrics for Analytical Chemistry*, 5th
49
50 edn, Pearson Prentice Hall, Gosport, 2005.
51
52
53
54
55
56
57
58
59
60

- 1
2
3
4
5
6
7
8
9
10
11
12
13
14
15
16
17
18
19
20
21
22
23
24
25
26
27
28
29
30
31
32
33
34
35
36
37
38
39
40
41
42
43
44
45
46
47
48
49
50
51
52
53
54
55
56
57
58
59
60
- 41 X. Fan, E. Roy, L. Zhu, T.C. Murphy, M. Kozlowski, M.S. Nanes and J. Rubin, *J. Biol. Chem.*, 2003, **278**, 10232-10238.
- 42 B.A. Trimmer, J.R. Aprille, D.M. Dudzinski, C.J. Lagace, S.M. Lewis, T. Michel, S. Qazi and R.M. Zayas, *Science*, 2001, **292**, 2486-2488.
- 43 M.D. Greenfiel, *Bioessays*, 2001, **23**, 992-995.
- 44 G.S. Timmins, F.J. Robb, C.M. Wilmot, S.K. Jackson and H.M. Swartz, *J. Exp. Biol.*, 2001, **204**, 2795-2801.
- 45 H. Ghiradella and J.T. Schmidt, *Integr. Comp. Biol.*, 2004, **44**, 203-212.
- 46 J.R. Aprille, C.J. Lagace, J. Modica-Napolitano and B.A. Trimmer, *Integr. Comp. Biol.*, 2004, **44**, 213-219.
- 47 H. van Lune and J.J. Bruggeman, Luciferase assay system, patent EP 1724359 A1.
- 48 W.M. Barnes and K.R. Rowlyk, Magnesium precipitate methods for magnesium dependent enzymes, U.S. patent application 2003/0027,196.
- 49 C. Little and P.J. O'Brien, *Eur. J. Biochem.*, 1969, **10**, 533-538.
- 50 S.M. Marques and J.C.G. Esteves da Silva, *Anal. Methods*, 2013, **5**, 1317-1327.
- 51 R. Fontes, D. Fernandes, F. Peralta, H. Fraga, I. Maio and J.C.G. Esteves da Silva, *FEBS J.*, 2008, **275**, 1500-1509.

Table 1 Commercial references of the enzymes used in the method

Enzyme	Source	EC	Product code	Lot
Glyceraldehyde 3-phosphate dehydrogenase	<i>Saccharomyces cerevisiae</i>	1.2.1.12	G5537	030M7715V
Phosphoglycerate kinase	<i>Saccharomyces cerevisiae</i>	2.7.2.3	P7634	061M7674V
Firefly luciferase	<i>Photinus pyralis</i>	1.13.12.7	L9506	060M7400
ATP sulfurylase	<i>Saccharomyces cerevisiae</i>	2.7.7.4	A8957	129K7680V
Inorganic pyrophosphatase	<i>Saccharomyces cerevisiae</i>	3.6.1.1	I1891	057K8618

Table 2 Center significance testing method results for the Plackett-Burman screening design

Factor	Effect in the presence of •NO 5 nM ^a
[Pi] / mM	--
[G3P] / mM	-
[NAD ⁺] / mM	NS
[ADP] / mM	++
[MgCl ₂] / mM	+
[Glycine] / mM	NS
[GAPDH] / μg mL ⁻¹	NS
[D-LH ₂] / μM	NS
[PGK] / μg mL ⁻¹	NS
[LUC] / μg mL ⁻¹	NS
Preincubation time / minutes	-

^a Significance of each effect at 95% level: NS, not significant; from + to +++, positive effect; from - to ---, negative effect.

Table 3 Analysis of Variance (ANOVA) table for the Box Behnken optimization design

	SS ^a	DF	MS	F-ratio	p-value	B-coefficient	SE _b
Summary							
Model	4.580 x 10 ⁵	20	2.290 x 10 ⁴	4.350	0.0004		
Error	1.263 x 10 ⁵	24	5.264 x 10 ³				
Adjusted total	5.843 x 10 ⁵	44	1.328 x 10 ⁴				
Variable							
Intercept	1.453 x 10 ⁶	1	1.453 x 10 ⁶	275.944	0.0000	539.000	32.447
[Pi] (A)	7.439 x 10 ³	1	7.439 x 10 ³	1.413	0.2462	-0.532	0.448
[G3P] (B)	0.250	1	0.250	4.749 x 10 ⁻⁵	0.9946	-0.185	26.872
[ADP] (C)	2.318 x 10 ⁵	1	2.318 x 10 ⁵	44.042	0.0000	743.055	111.967
[MgCl ₂] (D)	60.062	1	60.062	1.141 x 10 ⁻²	0.9158	0.567	5.304
Preincubation time (E)	1.665 x 10 ⁵	1	1.665 x 10 ⁵	31.622	0.0000	-13.600	2.418
AB	6.250	1	6.250	1.187 x 10 ⁻³	0.9728	-0.455	13.192
AC	650.250	1	650.250	0.124	0.7283	4.636	13.192
AD	156.250	1	156.250	2.968 x 10 ⁻²	0.8647	2.273	13.192
AE	1.225 x 10 ³	1	1.225 x 10 ³	0.233	0.6339	-6.364	13.192
BC	9.000	1	9.000	1.710 x 10 ⁻³	0.9674	0.545	13.192
BD	182.250	1	182.250	3.462 x 10 ⁻²	0.8540	-2.455	13.192
BE	16.000	1	16.000	3.039 x 10 ⁻³	0.9565	-0.727	13.192
CD	42.250	1	42.250	8.062 x 10 ⁻³	0.9294	-1.182	13.192
CE	121.000	1	121.000	2.299 x 10 ⁻²	0.8808	2.000	13.192
DE	25.000	1	25.000	4.749 x 10 ⁻³	0.9456	-0.909	13.192
AA	2.438 x 10 ³	1	2.438 x 10 ³	0.463	0.5026	-6.295	9.250
BB	4.975 x 10 ³	1	4.975 x 10 ³	0.945	0.3407	-8.992	9.250
CC	1.905 x 10 ⁴	1	1.905 x 10 ⁴	3.620	0.0692	-17.598	9.250
DD	1.415 x 10 ³	1	1.415 x 10 ³	0.269	0.6089	4.795	9.250
EE	2.649 x 10 ⁴	1	2.649 x 10 ⁴	5.032	0.0344	-20.750	9.250
Model check							
Main	4.058 x 10 ⁵	5	8.116 x 10 ⁴				
Int	2.433 x 10 ³	10	243.325	4.622 x 10 ⁻²	1.0000		
Int + squ	4.973 x 10 ⁴	5	9.947 x 10 ³	1.890	0.1336		
Squ	4.973 x 10 ⁴	5	9.947 x 10 ³		0.1336		
Error	1.263 x 10 ⁵	24	5.264 x 10 ³				
Lack of fit							
Lack of fit	1.201 x 10 ⁵	20	6.007 x 10 ³	3.879	0.0985		
Pure error	6.194 x 10 ³	4	1.549 x 10 ³				
Total error	1.263 x 10 ⁵	24	5.264 x 10 ³				

^a SS, Sum of squares; DF, degrees of freedom; MS, mean squares (ratio between SS and DF); *F*-ratio, ratio between ‘between-measures’ MS and ‘within-measures’ (residual) MS; *p*-value, probability of getting the *F*-ratio under the null hypothesis at 95%; *B*-coefficient, regression coefficient from a multiple linear regression analysis; SE_b, standard error of b.

Figures' captions

Scheme 1 Coupled enzymatic reactions. •NO, nitric oxide; G3P, glyceraldehyde 3-phosphate; Mg^{2+} , magnesium ions; GAPDH, glyceraldehyde 3-phosphate dehydrogenase; NAD^+ , β -nicotinamide adenine dinucleotide; Pi , phosphate ions; $\text{NADH} + \text{H}^+$, β -nicotinamide adenine dinucleotide (reduced form); 1,3-BPG, 1,3-bisphosphoglycerate; PGK, phosphoglycerate kinase; 3-PG, 3-phosphoglycerate; ADP-Mg^{2+} , adenosine 5'-diphosphate complexed with magnesium ions; ATP-Mg^{2+} , adenosine 5'-triphosphate complexed with magnesium ions; LUC, firefly luciferase; D-LH₂, firefly D-luciferin; O_2 , molecular oxygen; CO_2 , carbon dioxide; AMP-Mg^{2+} , adenosine 5'-monophosphate complexed with magnesium ions; PPi-Mg^{2+} , inorganic pyrophosphate complexed with magnesium ions; $h\nu$, photons; -SH, GAPDH thiol group; $-\text{S}^{\bullet}$, GAPDH thiyl radical.

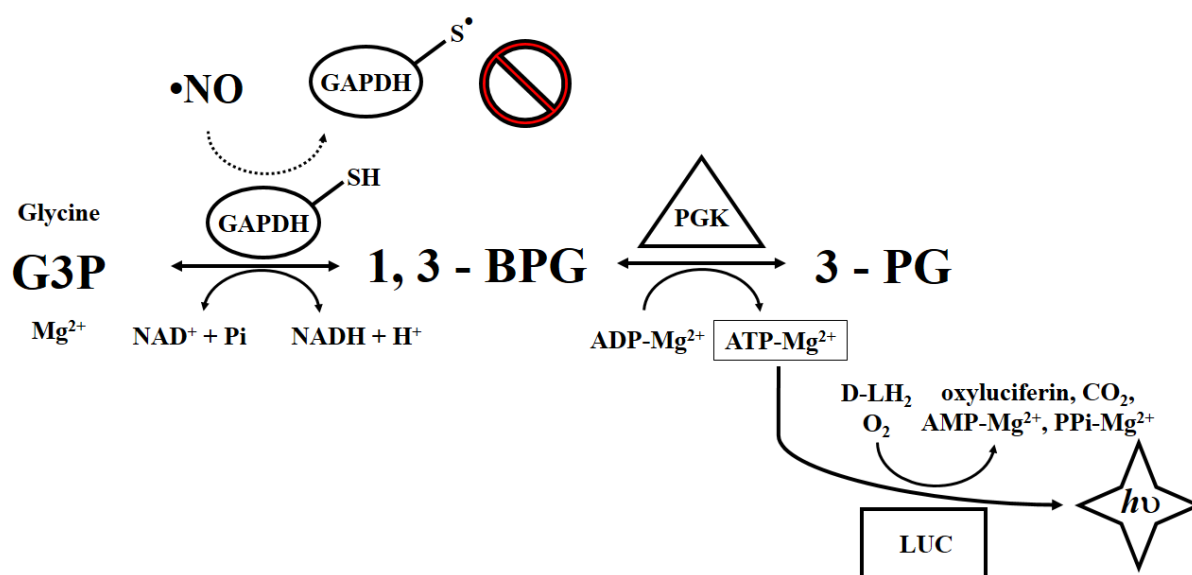
Scheme 2 Optimized coupled bioluminescent assay flowchart.

Fig. 1 Preliminary evaluation of the enzymatic reactions coupling and the effect of •NO on GAPDH. (A) Representative coupled bioluminescent assay luminograms and (B) the corresponding values of initial rate of bioluminescence generation. Positive controls were made in the absence of •NO, while negative controls were made in the absence of GAPDH. Asterisks indicate statistically significant difference as compared with the positive control ($p < 0.05$). The dashed lines in (A) indicate the linear portion of the luminograms, whose slopes correspond to the initial rates of bioluminescence generation (see Experimental section for further details). RLU, relative light units.

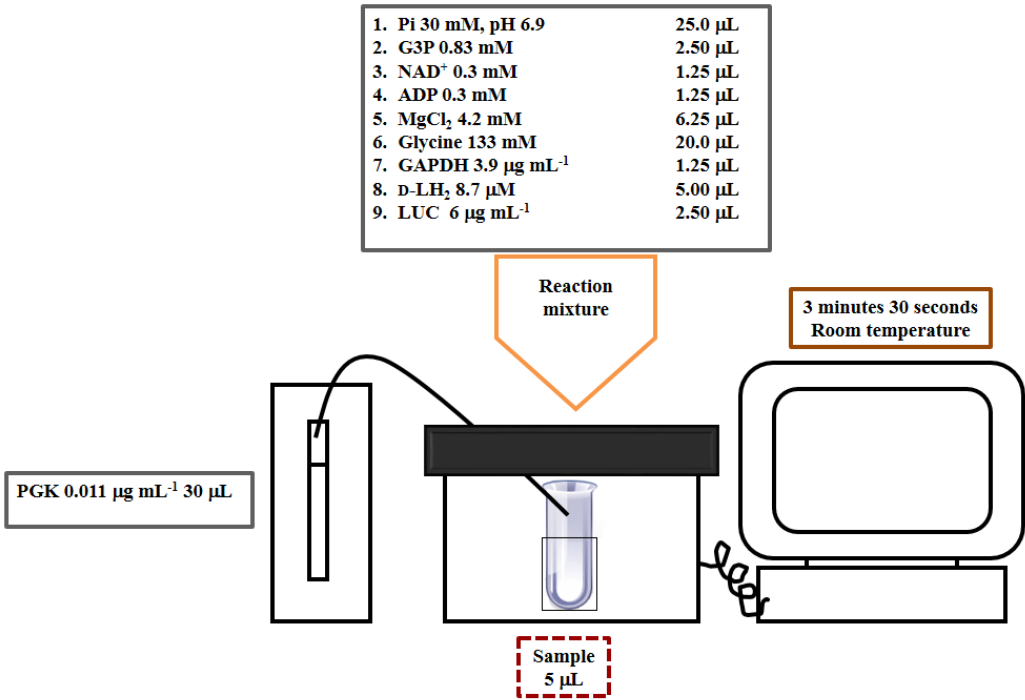
1
2
3
4
5
6
7
8
9
10
11
12
13
14
15
16
17
18
19
20
21
22
23
24
25
26
27
28
29
30
31
32
33
34
35
36
37
38
39
40
41
42
43
44
45
46
47
48
49
50
51
52
53
54
55
56
57
58
59
60

Fig. 2 Representative exploratory curve for •NO. *Inset* Amplification of the zone with linear response. RLU, relative light units.

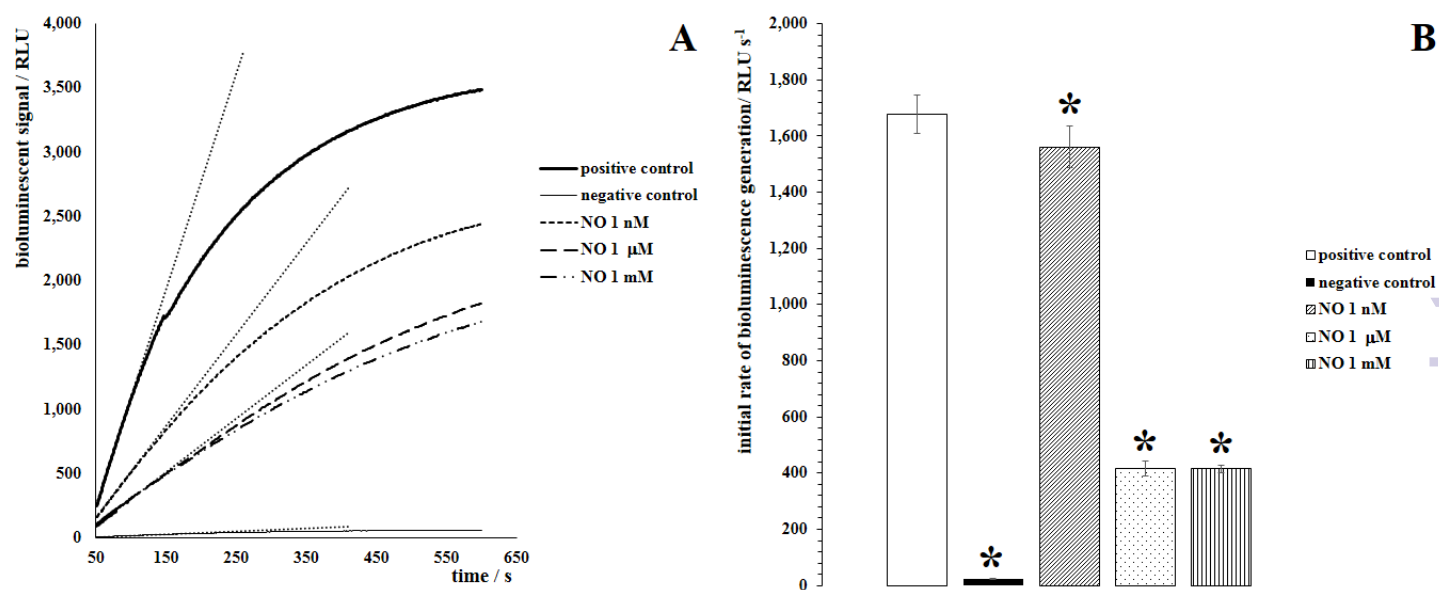
Fig. 3 Representative standard additions curve for the •NO assay in microalgae culture medium. RLU, relative light units.



Scheme 1



Scheme 2



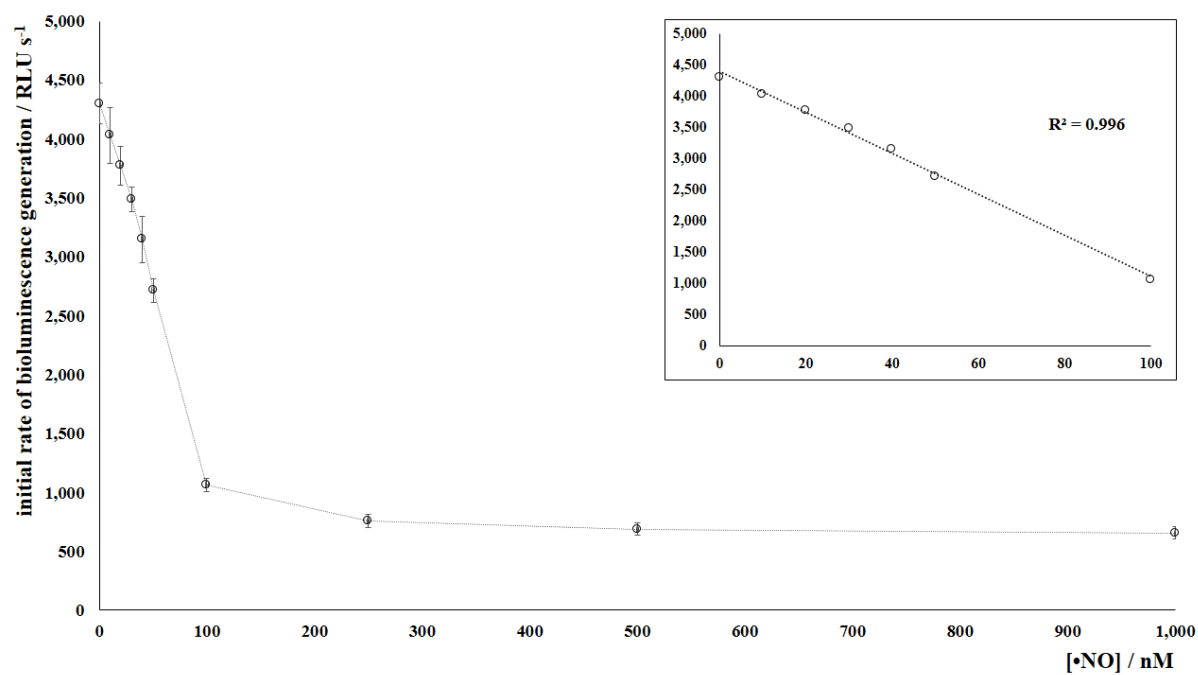
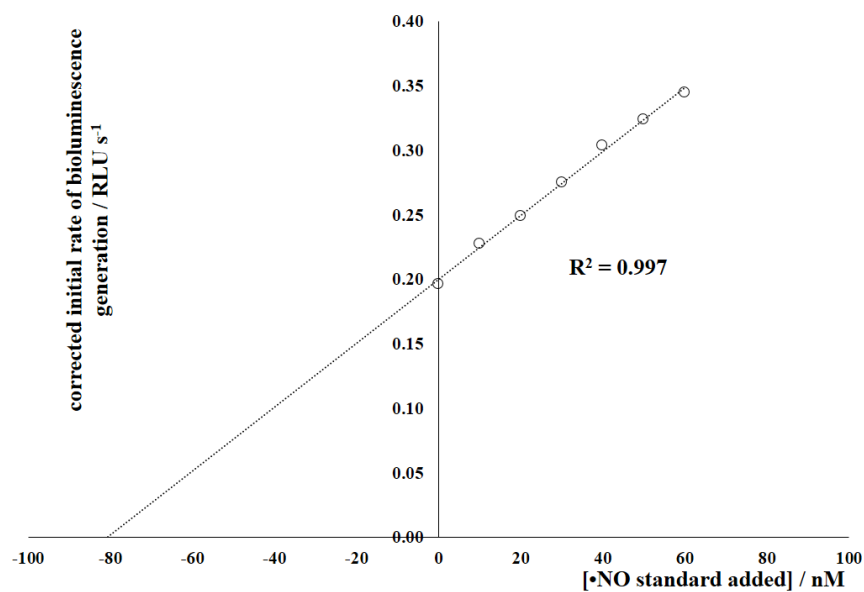


Fig. 2

**Fig. 3**